Published in final edited form as:

NMR Biomed. 2015 November ; 28(11): 1518–1525. doi:10.1002/nbm.3411.

In vivo quantification of hyperoxic arterial blood water T_1

Jeroen C.W. Siero[1,*], **Megan K. Strother**[2,3], **Carlos C. Faraco**[2], **Hans Hoogduin**[1], **Jeroen Hendrikse**[1], and **Manus J. Donahue**[2,4,5]

[1]Radiology, University Medical Center Utrecht, Utrecht, The Netherlands [2]Radiology and Radiological Sciences, Vanderbilt Medical Center, Nashville, TN, USA [3]Neurological Surgery, Vanderbilt Medical Center, Nashville, TN, USA [4]Neurology, Vanderbilt Medical Center, Nashville, TN, USA [5]Psychiatry, Vanderbilt Medical Center, Nashville, TN, USA

Abstract

Hyperoxic and hypercapnic hyperoxic gas challenges are increasingly being used in cerebrovascular reactivity (CVR) and calibrated fMRI experiments. The longitudinal arterial blood-water relaxation time (T_{1a}) change with hyperoxia will influence signal quantification through mechanisms relating to elevated partial pressure of plasma-dissolved O_2 (pO_2) and increased oxygen bound to hemoglobin in arteries (Y_a) and veins (Y_v). The dependence of T_{1a} on Y_a and Y_v has been elegantly characterized *ex vivo*, however the combined influence of pO_2, Y_a and Y_v on T_{1a} *in vivo* under normal ventilation have not been reported. Here, T_{1a} is calculated during hyperoxia *in vivo* by a heuristic approach that evaluates T_1-dependent arterial spin labeling (ASL) signal changes to varying gas stimuli. Healthy volunteers (n=14; age=31.5±7.2yrs) were scanned using pseudo-continuous ASL in combination with room air (RA;21%O_2/79%N_2), hypercapnic-normoxic (HN; 5%CO_2/21%O_2/74%N_2), and hypercapnic-hyperoxic (HH; 5%CO_2/95%O_2) gas administration. HH T_{1a} was calculated by requiring that the HN and HH CBF change be identical. The HH protocol was then repeated in patients (n=10; age=61.4±13.3yrs) with intracranial stenosis to assess whether a HH T_{1a} decrease prohibited ASL from being performed in subjects with known delayed blood arrival times. Arterial blood T_{1a} decreased from 1.65s at baseline to 1.49±0.07s during HH. In patients, CBF values in the affected flow territory for the HH condition were increased relative to baseline CBF values and were within physiological range (RA-CBF=36.6±8.2ml/100g/min;HH-CBF=45.2±13.9ml/100g/min).

Conclusion—Hyperoxic (95% O_2) 3T arterial blood T_{1aHH} =1.49±0.07s relative to a normoxic T_{1a} of 1.65s.

Graphical Abstract

Correspondence to: Jeroen C.W. Siero.

[*]**Present address:** UMC Utrecht, Dept of Radiology, Room Q02.4.310, Heidelberglaan 100, 3508 AG, Utrecht, Netherlands, tel. +31 88-7553262, j.c.w.siero@umcutrecht.nl

Declaration of conflict of interest: The authors declare that no conflict of interest exists

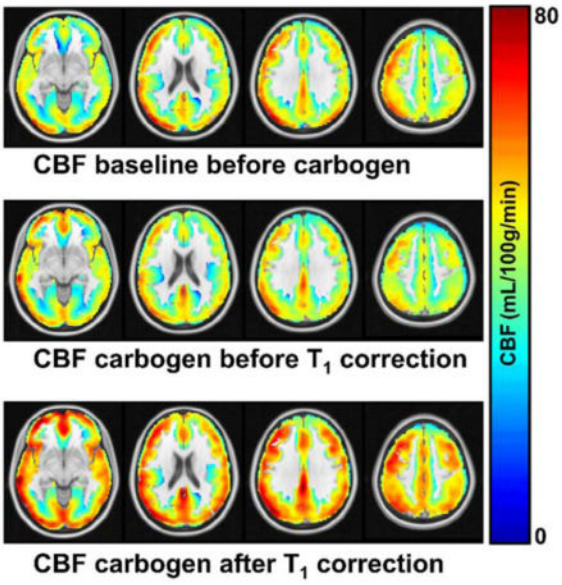

We calculate in vivo arterial blood T_1 changes at 3T during hyperoxic hypercapnic (carbogen) gas challenges.

A heuristic approach was used to compute T_1-dependent ASL signal changes to varying gas stimuli.

Arterial blood T_1 decreased from 1.65s at baseline to 1.49 ± 0.07s during carbogen.

The T_1 correction was applied to ASL data in intracranial stenosis patients using a carbogen protocol.

The calculated T_1 value should provide reference for future calibrated fMRI, ASL and VASO experiments using hyperoxic gas mixtures.

Keywords

carbogen; arterial spin labeling; blood; hypercapnia; cerebrovascular reactivity; hyperoxia; T_1

Introduction

Cerebrovascular reactivity (CVR) can be defined as the change in cerebral blood flow (CBF) and volume (CBV) in response to a vascular stimulus, and can be used to examine vascular reserve capacity or iso-metabolic reactivity mechanisms. Breathing hypercapnic gas mixtures causes relaxation of arteriolar smooth muscles through mechanisms related to reductions in pH, which in turn cause global increases in CVR in gray and white matter parenchyma (1,2). As such, a non-invasive method for eliciting CVR changes is with the administration of hypercapnic gas mixtures (e.g., CO_2 in air: 5% CO_2/21% O_2/74% N_2 or carbogen-5: 5% CO_2/95% O_2), which both allow for evaluation of vascular compliance in health and disease (3–8).

The elicited changes in CVR can be measured with non-invasive MRI techniques, the most common being blood-oxygenation-level-dependent (BOLD) MRI. However, the BOLD signal is nonspecific, influenced by CBF, CBV and cerebral metabolic rate of oxygen consumption ($CMRO_2$), and deciphering the contributions of each is non-trivial. An alternative MRI technique is arterial spin labeling (ASL) (9). ASL MRI is more specific to CBF by magnetically labeling the arterial blood water proximal to the imaging region and acquiring an image after a post-labeling delay (PLD) time. This labeled image is subtracted from a non-labeled or "control" image, resulting in a CBF-weighted image. One difficulty with ASL and hyperoxia is that the label decays with the arterial blood water T_{1a}. The T_{1a} is highly dependent on blood oxygenation status, which will influence the measured CBF if not incorporated correctly into quantification models.

T_{1a} values for different O_2 saturation (fraction of O_2 bound to hemoglobin) levels have been estimated *ex vivo* in bovine blood at 3T (10,11), 4.7T (12) and 7T (13), and human blood (14). The disadvantage of *ex vivo* experiments is that anti-coagulants added to the blood mixtures may influence relaxation mechanisms while it is also difficult to precisely control for temperature, O_2 saturation, and pO_2 at physiological levels in all experiments. *In vivo* estimation of T_{1a} is likewise challenging due to both practical issues and two competing physiological effects that influence blood water T_1 during hyperoxia (12,15). First, hyperoxia increases arterial and venous O_2 saturation (Y_a and Y_v, respectively) which will increase blood water T_1 due to paramagnetic effects from decreased deoxyhemoglobin content. Previous *ex* vivo work has shown that blood water $R_1 = 1/T_1$ decreases linearly with increasing hemoglobin O_2 saturation (12,13). Second, hyperoxia also increases the arterial and venous partial pressure of O_2 (P_aO_2 and P_vO_2, respectively) and thus the amount of plasma dissolved O_2, resulting in a decrease in blood water T_1. Previous *ex vivo* work has shown that $R_1 = 1/T_1$ increases linearly with plasma dissolved O_2 concentration (11,12).

A practical drawback of *in vivo* T_{1a} estimation using multi-recovery or multi-flip angle approaches is primarily that it is difficult to localize pure blood voxels, especially arterial blood voxels, and additionally that blood may flow in or out of the inversion/excitation volume over the experiment, thereby complicating steady state assumptions (16–20). Additionally, the presence of inhomogeneous B_0 and B_1 fields can complicate quantification. Previous *in vivo* studies have focused mainly on measuring venous blood water T_{1v} to circumvent the issues, as venous blood water in the superior sagittal sinus can be inverted over a larger spatial range of homogenous B_0 and B_1 and also the sagittal sinus is large enough to enable blood voxels to be isolated with minimal partial volume effects (16–20). Using T_{1v} as a proxy for studying the effect of hyperoxia on T_{1a} is complicated by the previously mentioned two effects that influence blood water T_1. During hyperoxia, venous blood undergoes a more complicated process as it will see a substantial increase in Y_v (as compared to Y_a) and thus an increase in T_{1v}. This effect is known to be the dominant effect compared to the decrease in T_{1v} due to the small increase in plasma-dissolved O_2 (P_vO_2) (21).

In general, *ex vivo* and *in vivo* studies indicate that the prominent T_{1a} effect of hyperoxia occurs from increases in plasma dissolved O_2 resulting in an overall decreased T_{1a} (12–15,18). One study investigated the CBF response in humans to hyperoxia using ASL MRI at

3T (15) and obtained T_{1a} values using extrapolation of *ex vivo* literature values (10) for a range of O_2 saturation levels. To our knowledge, the T_{1a} value at 3T for hyperoxic blood conditions has not been experimentally quantified *in vivo*. As the T_{1a} affects the decay of the label and thus the CBF quantification, the issue is fundamental to CBF measurements using hyperoxia in basic science (10,15,22–26) but also in clinical studies, for example CVR evaluations in steno-occlusion patients (5,27,28). In the latter, a hyperoxic component may be incorporated to increase tissue or blood oxygenation for the purposes of extracting additional information regarding blood arrival times, blood volume, and/or metabolism (1,3,29–33). Knowledge of T_{1a} is equally important in calibrated fMRI experiments. These incorporate ASL and BOLD imaging to estimate neuronal induced $CMRO_2$ changes using hybrid (hypercapnic and hyperoxic) gas challenges (8). Furthermore, for studies using vascular space occupancy (VASO) MRI (34,35) combined with hypercapnic/hyperoxic gas challenges, accurate knowledge of T_{1a} for different conditions is crucial for precise nulling of arterial blood and thus quantification of CBV changes.

Here, we utilize quantification principles of ASL and the dependence of this contrast on T_{1a} to quantify T_{1a} *in vivo*. To achieve this, we apply hypercapnic normoxia ($5\%CO_2/21\%O_2/74\%N_2$, abbreviated as HN) and hypercapnic hyperoxia ($5\%CO_2/95\%O_2$, i.e. carbogen-5, abbreviated as HH) stimuli sequentially in healthy volunteers in conjunction with ASL MRI. The hypothesis to be investigated is that when there is a small-to-negligible effect on CBF of breathing hyperoxia for short durations (33,36,37), it is possible to quantify the T_{1a} change during carbogen administration. Here the assumption is that the identical hypercapnic fraction (i.e., 5% CO_2) is the predominant contributor to CBF changes in both stimuli types, HN and HH, and thus CBF changes should be similar between these two stimuli after controlling for T_{1a} changes. Nonetheless, to accommodate any potential CBF changes of hyperoxia, we also computed the $T_{1a,HH}$ for a range of simulated hyperoxia induced CBF changes.

Finally, we assess the clinical feasibility of ASL in the presence of hyperoxia by applying the calculated hyperoxic T_{1a} to ASL data acquired during HH administration in patients with angiographically-confirmed stenosis with delayed blood water transit times (38,39). The purpose of this component of the study was to evaluate whether decreases in $T_{1a,HH}$ prohibited pCASL data from being interpretable during HH administration at typical PLD times. This possibility exists owing to the faster recovery of the longitudinal component of blood water magnetization following inversion in the presence of hyperoxia, which may lead to insufficient SNR at typical PLDs in patients with delayed bolus arrival time, thereby providing non-physiological CBF values and/or CBF reactivity measures.

Materials and Methods

Participants

Healthy volunteers (n = 14; 8M/6F; age = 31.5 ± 7.2 yrs) with no history of cerebrovascular disease or stroke and subjects (n = 10; 6M/4F; age = 61.4 ± 13.3 yrs) with angiographically-confirmed intracranial (IC) stenosis provided informed, written consent. The study was approved by the Institutional Review Board and in compliance with the Helsinki Declaration.

Arterial blood water T_1 quantification procedure

Healthy volunteers were scanned on a 3T Philips Achieva system (Philips Healthcare, Best, The Netherlands) using body coil transmission and 8-channel SENSE head coil reception. Participants were closely fitted with a non-rebreathing oxygen mask and a nasal cannula. Gas was delivered to the mask at 12L/min during a breathing protocol of baseline period (room air, RA) followed by hypercapnic gas mixture period (either 5% CO_2 in air, HN; or carbogen-5, HH). Stimulus order was randomized across participants, and heart rate, Y_a, and end-tidal CO_2 ($EtCO_2$) were required to return to baseline before beginning the next scanning block presentation (approximately 3 min). CBF changes were assessed using pseudo-continuous ASL (pCASL) with a multi-slice single-shot EPI readout. Healthy volunteers were split in two groups ($n_1 = 7$ and $n_2 = 7$) and scanned with two different gas administration period durations and PLD times to evaluate whether small variations in blood transit time between gas stimuli did not contribute substantially to the $T_{1a,HH}$ measurement.

Group 1 ($n_1 = 7$, 4M/3F; age = 33.6 ± 9.4 years) was subjected to a 272.5s baseline RA period followed by a 272.5s gas mixture (HN or HH) period. Group 1 pCASL scan parameters were: TR=3900ms, TE=13ms, PLD=1525ms, background suppression was enabled, spatial resolution=3.5×3.5×7mm^3, inter-slice gap=0.5 mm, slices=17, volumes=27 (RA + HH/HN), scan duration=545s. Spin labeling was performed using a label-duration of 1.5s consisting of 0.5 ms Hanning-windowed pulses. Group 2 ($n_2 = 7$, 4M/3F; age = 29 ± 3.7 years) was subjected to a 240s baseline RA period followed by a 240s gas mixture (HN or HH) period. Group 2 pCASL scan parameters were identical to group 1 except: PLD=1700ms; spatial resolution = 3.5×3.5×7mm^3, inter-slice gap=0.5 mm, volumes = 13 (for both RA and HH/HN), scan duration = 109s.

The pCASL scans were started when the observed $EtCO_2$ level plateaued. The experimental design is shown in Figure 1A.

Additionally, an M_0 scan was acquired for both groups for CBF quantification, using identical acquisition geometry as the pCASL scan but with a TR=20s and 15s for group 1 and group 2, respectively, and the spin labeling pulse-train turned off.

Data were corrected for motion using standard routines from the FMRIB Software Library (FSL (40)). CBF in both RA conditions and both HN and HH stimulus blocks was quantified by applying a simplified single-compartment pCASL kinetic model as recently suggested by the ISMRM perfusion study group and ASL white paper (41) to the average difference magnetization (ΔM). The ΔM data was obtained using a surround-subtraction approach that also realizes baseline drift removal. CBF was quantified according to

$$\mathrm{CBF_i} = \frac{6000 \cdot \lambda \cdot \Delta \mathrm{M} \cdot \mathrm{e}^{\mathrm{PLD}/\mathrm{T_{1a,i}}}}{2\alpha \mathrm{M_0}.\mathrm{T_{1a,i}} \cdot \left(1 - \mathrm{e}^{-\tau/\mathrm{T_{1a,i}}}\right)} \quad [1]$$

for i = RA, HN, or HH,

where CBF is in ml/100g/min, $\alpha = 0.85$ is the pCASL labeling efficiency, $\tau = 1.5$s is the labeling duration, T_{1a} is the arterial blood water T_1 (in seconds), and $\lambda = 0.9$ml/g is the

tissue/blood partition coefficient of water. M_0, the equilibrium brain magnetization signal, was obtained from the equilibrium M_0 scan after spatial smoothing using a 3-dimensional Gaussian kernel (full-width-half-at-maximum = 7mm). *PLD* is 1.525s and 1.700s for group 1 and group 2, respectively. The slice dependency of the PLD was taken into account using the slice time of the pCASL scan.

CBF in the RA, HN and HH conditions was initially quantified using Eq. 1 assuming a $T_{1a,RA} = T_{1a,HN} = T_{1a,HH,initial}$ = 1.65s measured *ex vivo* under normoxic conditions from bovine blood water (10). Also, this value is recommended by the ISMRM perfusion study group and ASL white paper (41), and therefore expected to be used abundantly in future ASL-based CBF studies as reference $T_{1a,RA}$ value. CBF data were spatially smoothed using a 3-dimensional Gaussian smoothing kernel (full-width-half-at-maximum=7 mm) and registered to MNI standard space using the FLIRT tool from FSL (40). Subsequent processing was done in MATLAB (Mathworks, Natick, MA). We focused on cortical gray matter CBF (using a cortical gray matter MNI mask) as white matter CBF transit time is 2–3 times longer than gray matter and thus could not be accurately sampled at our PLD (42).

To determine the $T_{1a,HH}$, the parameter of interest, we required that the mean HN and HH cortical CBF change, ΔCBF, relative to RA be identical. This heuristic approach assumes that the vasodilatory effect from hypercapnia is much greater than any small vasoconstrictive effects that may occur during a short period of hyperoxia. The CBF for the HH condition was recomputed for a range of $T_{1a,HH}$ values; 1.3s to 1.62s in steps of 0.004s, yielding a calibration curve of the ΔCBF dependency on $T_{1a,HH}$. Also, to accommodate different assumed normoxic $T_{1a,RA}$ values in future studies we repeated the above simulation for a range of different *normoxic* $T_{1a,RA}$ (and thus $T_{1a,HN}$) values: 1.6 to 1.75s in steps of 0.01s.

Lastly, to investigate potential hyperoxic vasoconstrictive effects, we simulated how the calculated $T_{1a,HH}$ values would change for small reductions (0%–20%) in HH CBF relative to HN CBF. The following model was used:

$$\mathrm{CBF}_{HH} = (1-c) \cdot \mathrm{CBF}_{RA} + \Delta\mathrm{CBF}_{HH} \quad [2]$$

where *c* is the fractional reduction, ranging from 0 to 0.2, in baseline (RA) CBF due to hyperoxic vasoconstriction, and ΔCBF_{HH} the absolute increase in CBF due to hypercapnic vasodilation (assumed to be identical for both HN and HH conditions).

A $T_{1a,HH}$ value for each participant and each normoxic $T_{1a,RA}$ was computed, and averaged to arrive at a group mean $T_{1a,HH}$ value, for group 1 and group 2 respectively, and a total mean $T_{1a,HH}$ across both groups. Using the total mean $T_{1a,HH}$, the HH CBF was quantified again for each volunteer. Comparisons were made between the CBF values for the two baseline RA conditions, and between the corrected CBF values in the HH condition vs CBF values in the HN condition, using two-tailed Student's t-tests with Bonferroni correction for two comparisons (uncorrected $p = 0.05$; corrected $p = 0.025$).

Intracranial stenosis study

Patients with flow-limiting IC stenosis of at least one major IC vessel (e.g., middle cerebral artery, MCA; posterior cerebral artery, PCA; anterior cerebral artery, ACA; or intracranial segments of the internal carotid artery, ICA) received an identical HH protocol as in the healthy volunteer study outlined above.

Data were collected and managed using REDCap electronic data capture tools (16). Stenoses were measured by board-certified neuroradiologist (MKS; experience = 11 years) from clinically acquired computerized tomography angiography (CTA), digital subtraction angiography (DSA), or magnetic resonance angiography (MRA) according to criteria in Samuels et al. (43) for IC stenosis, and according to the North American Symptomatic Carotid Endarterectomy Trial (NASCET) criteria in the case of extracranial stenosis (44). Inclusion criteria were that patients had intracranial stenosis greater than 50%. The $T_{1a,HH}$ correction of the CBF HH patient data was performed using the $T_{1a,HH}$ estimated from the healthy volunteers. CBF data were averaged for each condition (RA, $T_{1a,HH}$ corrected HH and uncorrected HH), and CBF values were compared (corrected HH vs RA; corrected HH vs uncorrected HH) using two-tailed Student's t-tests with Bonferroni correction for two comparisons (uncorrected $p = 0.05$; corrected $p = 0.025$).

Results

In healthy controls (Figure 1B) cortical CBF values for RA conditions before HN (mean ±s.d. = 40.9 ± 6.1 ml/100g/min) and before HH (mean±s.d. = 42.3 ± 7.7 ml/100g/min) did not significantly differ ($p = 0.17$). As expected by the current approach for computing the $T_{1a,HH}$ values, the corrected CBF values for the HH condition (mean±s.d. = 49.3 ± 9.5 ml/100g/min) did not significantly differ from the CBF values for the HN condition (mean±s.d. = 47.7 ± 8.2 ml/100g/min; $p = 0.25$). Similarly, a significant correlation was found between corrected ΔCBF_{HH} and ΔCBF_{HN} (Pearson $R^2 = 0.51$, $p = 0.0046$). No significant difference was found between end-tidal CO_2 changes ($p = 0.17$, two-tailed paired Student's t-test) for the HN and HH condition between subjects (mean ± s.d. $\Delta EtCO_2 = 6.8 \pm 2.0$ and 5.6 ± 3.4 mmHg for the HN and HH condition respectively). Note that the uncorrected HH CBF (mean±s.d. = 41.8 ± 8.2 ml/100g/min) was not significantly different ($p = 0.67$) from the RA condition, demonstrating that the $T_{1a,HH}$ has a large effect on CBF quantification. Group CBF maps for healthy volunteers are shown in Figure 2.

In patients (Figure 1C, Table 1), the corrected HH CBF values (mean±s.d.= 45.2 ± 13.9 ml/100g/min) did significantly differ ($p < 0.005$) from both the RA condition (mean±s.d.= 36.6 ± 8.2 ml/100g/min) and the uncorrected HH condition (mean±s.d.= 38.4 ± 11.8 ml/100g/min). Note that the uncorrected HH and RA CBF values did not significantly differ ($p = 0.32$). Group CBF maps for patients are shown in Figure 3.

The mean $T_{1a,HH}$ value (Figure 4A) calculated in the HH condition across both groups was 1.49 ± 0.07s (with mean±s.d 1.48 ± 0.08s and 1.50 ± 0.06s for group 1 and group 2, respectively). The $T_{1a,HH}$ value between the two groups did not differ significantly ($p = 0.6$). The dependency of ΔCBF_{HH} ($CBF_{HH} - CBF_{RA}$) is well approximated by a quadratic decreasing function with respect to $T_{1a,HH}$ and a quadratically increasing function with

respect to assumed normoxic $T_{1a,RA}$ (Figure 4B). The reduction of the calculated $T_{1a,HH}$ for different assumed normoxic $T_{1a,RA}$ is fairly constant; a mean±s.d. T_1 reduction of 162 ± 8ms across a range, 1.60 – 1.75s, of $T_{1a,RA}$ values was computed (Figure 4C).

Figure 5 shows how the $T_{1a,HH}$ would change if the hyperoxic component of the HH mixture had a small-to-moderate (0 – 20%) vasoconstrictive effect on reducing baseline CBF. To completely attribute the reduced CBF in the HH condition to vasoconstrictive effects, thus no hyperoxic T_1 effect ($T_{1a,HH} = T_{1a,RA} = 1.65$s), a ~16% CBF reduction is necessary. This is approximately the same percentage difference between the uncorrected and corrected HH CBF values (Figure 1B), as expected.

Discussion

The overall finding from this work is that carbogen-5 (hypercapnic hyperoxia, HH) results in a $T_{1a,HH}$ of approximately 1.49s in humans, relative to a normoxic baseline $T_{1a,RA}$ of 1.65s. This value may be useful for quantitative ASL experiments that implement hyperoxic gas challenges such as the recently proposed calibrated BOLD model using hybrid gas challenges (8). Also other functional imaging approaches using hyperoxic gas challenges, such as vascular space occupancy (VASO) MRI (34) will benefit from accurate knowledge of $T_{1a,HH}$ to more precise blood nulling. The $T_{1a,HH}$ results presented in this work are valid for hypercapnic gas mixtures containing 95% O_2 content. As previous *ex-vivo* studies have shown a linear dependency of $R_{1,a} = 1/T_{1,a}$ with O_2 concentration (pO_2) (11,12), we suggest that extra- and interpolation of our results can be used for other amounts of O_2 content.

Not surprisingly, subject variability of the $T_{1a,HH}$ value was observed. Our fitting approach is likely affected by the relatively large spatial resolution which can introduce partial volume effects between white and gray matter, CSF, and vascular compartment (e.g., arteriole vs. venules), and as such different voxels are anticipated to respond differently to vasoactive stimuli. However this bias is similar between all subjects in both groups studied as evidenced by the relatively similar calculated $T_{1a,HH}$ between subjects of the two groups (Figure 4A).

Analysis of the patient data supports the clinical feasibility of using hyperoxic gas challenges with ASL sequences, even in patients with known steno-occlusive disease. It is well-known that CBF increases after carbogen-5 (HH) administration (6,33). This change is only present when incorporating appropriate $T_{1a,HH}$ values in the quantification model (Figure 3). Due to the complicated nature of CBF in patients with atherosclerosis and the heterogeneity of stenosis locations in this patient group, changes in CBF across affected and unaffected regions were not evaluated. With a larger patient cohort, CBF reactivity comparisons across affected and unaffected regions could be of interest for future research.

A confounding factor of the analysis could be the interplay of hypercapnia and hyperoxia (vasodilation vs. vasoconstriction) and the resulting influence on CBF, as we assume here that short durations of hyperoxia have a negligible effect on CBF relative to the accuracy of the ASL measurement and relative to hypercapnia. The effect of hyperoxia on CBF remains a controversial topic as contradicting results have been reported (15,22,36,37,45–47) and

thus it becomes difficult to confidently argue that there is indeed a small-to-negligible effect on CBF. Reasons for a reduction in CBF are a potential direct vasoconstrictive effect of O_2 and hyperventilation (increased expired ventilation volume per minute) that causes P_aCO_2 to decrease (22). Several ASL-based studies have observed a slight reduction in CBF when breathing hyperoxic gasses (on the order of 2–10% reduction upon 5–12 min. of 100% O_2) (15,29,37,45). For instance, a very small CBF decrease (~2% for gray matter) was reported using ASL at 1.5T, however this was not significantly different from zero (37) when using a corrected $T_{1a,HH}$ measured in non-cerebral body regions(18,21). Other ASL studies did find a significant decrease in CBF of ~10% at 3T (15) and ~30% at 1.5 T (22). The latter study however used a fixed T_{1a} for both room air and hyperoxic conditions. Independent [^{15}O]-H_2O PET work in humans has revealed a non-significant but trending decrease in CBF during much longer durations (10 min) of hyperoxia (100% O_2) for healthy volunteers of about 3 mL/100g tissue/min, and non-significant mean CBF changes in steno-occlusive patients (33). Phase-contrast based MRI studies also reported a slight CBF reduction during hyperoxia (46,47), however a correction for the confounding decrease in P_aCO_2 due to hyperventilation of hyperoxia was not performed. A more recent phase-contrast MRI study by Xu et al. did correct for P_aCO_2 changes during hyperoxia which resulted in a non-significant CBF decrease (36). In this study, to accommodate any possible CBF changes of hyperoxia, we therefore computed the $T_{1a,HH}$ for a range of simulated hyperoxia induced CBF changes. Figure 5 demonstrates how the calculation of $T_{1a,HH}$ would change if transient hyperoxia reduced CBF. The $T_{1a,HH}$ value calculated here (1.49s at 95%O_2, assuming a normoxic $T_{1a,RA}$ of 1.65s) may be underestimated if hyperoxia leads to substantial CBF decreases. In general, more work is needed to elucidate the effect of hyperoxia on cerebral blood flow using either stable direct T_{1a} measurements or T_1 independent methods such as phase-contrast MRI or PET. Dynamic susceptibility contrast MRI using a multi-echo readout to isolate T_2* changes might also be an option, however, this would require injection of an exogenous contrast agent (gadolinium). Of importance is also to study the effect of the O_2 content amount and stimulus duration in order to give an exemplar for an optimal hyperoxic-stimulus protocol where hyperoxic induced CBF changes are minimal.

Another confound is that our approach relies on the single-compartment kinetic model (41). Here a single T_1 value (arterial blood with a single P_aO_2 value) is used to describe the ASL signal in a voxel, and it assumes that the blood-tissue water exchange is almost instantaneous. A more likely scenario is that the labeled blood experiences a range of P_aO_2 values and may even reach the more venous side in the capillary bed. Therefore, a continuum of T_{1a} values is experienced which should ideally be incorporated in the ASL signal model. Furthermore, bolus arrival times are regionally dependent and, like the pCASL labelling efficiency, dependent on hypercapnic state (26,48). This will also affect the CBF quantification and the continuum of T_{1a} values the blood experiences in the cerebral vasculature. Another matter is the complex biochemistry of carbogen as it affects both the O_2 and CO_2 hemoglobin dissociation curves through the Bohr and Haldane effects (25). Hyperoxia will facilitate CO_2 unloading (Haldane effect), thus increasing local P_aCO_2, whereas hypercapnia will facilitate O_2 unloading (Bohr effect), thus increasing local P_aO_2. However, due to the combined hypercapnic and hyperoxic state it is not unlikely that the

Bohr and Haldane effects are partially negated. For example, the increased hemoglobin O_2 unloading due to hypercapnia (Bohr effect) can be partially restored by the increased P_aO_2 due to hyperoxia, and vice versa for the Haldane effect. These effects have recently been simulated by Faraco et al (49).

In conclusion, while the calculated $T_{1a,HH}$ could be adjusted for slight vasoconstrictive effects of hyperoxia, this value is slightly longer than previously computed $T_{1a,HH}$ values at 3T using extrapolation (~1.38s) (15) and *ex vivo* estimation using bovine blood (~1.45s, for 95% O_2) (11), and therefore suggests a slower recovery of the labelled blood under hyperoxic conditions than may have been assumed previously. Only after incorporating the adjusted $T_{1a,HH}$ value in a ASL CBF quantification model, hypercapnic induced CBF changes were observed in patients with known steno-occlusive disease. This shows the feasibility of using hypercapnic-hyperoxic gas mixtures in ASL-based CBF studies. The $T_{1a,HH}$ value reported here (in-vivo at 3T for 95% O_2) together with a 'calibration curve' for different assumed normoxic T_{1a} and vasoconstrictive effects can be of significance for future studies. More work, however, is warranted to thoroughly characterize the dependence of CBF changes for different hyperoxic stimulation durations and inspired O_2 content. The $T_{1a,HH}$ value calculated here should provide a reference for future calibrated BOLD fMRI, VASO and ASL-based CVR experiments using hyperoxic gas mixtures.

Acknowledgments

Funding: The authors would like to thank Dave Pennel, Lindsey Dethrage, Leslie McIntosh, Kristen George-Durrett, Paul Clemmons, and Diane Brown for experimental support, as well as the National Institute of Neurological Disorders and Stroke (NINDS) for funding (NIH/NINDS 5RO1NS078828) and the American Heart Association (14CSA20380466). Jeroen Hendrikse was supported by European Research Council (ERC) grant number: ERC-2014-StG - 637024_HEARTOFSTROKE.

List of Abbreviations

ΔM	difference magnetization
ACA	anterior cerebral artery
ASL	arterial spin labeling
BOLD	blood oxygenation level-dependent
CBF	cerebral blood flow
CBV	cerebral blood volume
CTA	computerized tomography angiography
CVR	cerebrovascular reactivity
DSA	digital subtraction angiography
EtCO2	end-tidal CO_2
FLIRT	FMRIB's Linear Image Registration Tool
FMRIB	Functional MRI of the Brain Centre

FSL	FMRIB Software Library
Hct	Hematocrit
HH	hypercapnic hyperoxia
HN	hypercapnic normoxia
IC	intracranial
ICA	internal carotid artery
ISMRM	International Society for Magnetic Resonance in Medicine
MCA	middle cerebral artery
MNI	Montreal Neurological Institute
MRA	magnetic resonance angiography
NASCET	North American Symptomatic Carotid Endarterectomy Trial
PaO_2	arterial partial pressure of oxygen
PCA	posterior cerebral artery
pCASL	pseudo-continuous arterial spin labeling
PET	positron emission tomography
PLD	post-labeling delay
pO_2	partial pressure of oxygen
PvO_2	partial pressure of venous oxygen
RA	room air
SNR	signal to noise ratio
VASO	vascular space occupancy
Y_a	arterial oxygen saturation fraction
Y_v	venous oxygen saturation fraction

References

1. Ashkanian M, Borghammer P, Gjedde A, Østergaard L, Vafaee M. Improvement of brain tissue oxygenation by inhalation of carbogen. Neuroscience. 2008; 156:932–938. [PubMed: 18786619]
2. Ito H, Kanno I, Ibaraki M, Hatazawa J, Miura S. Changes in human cerebral blood flow and cerebral blood volume during hypercapnia and hypocapnia measured by positron emission tomography. J Cereb Blood Flow Metab. 2003; 23:665–70. [PubMed: 12796714]
3. Wise RG, Harris AD, Stone AJ, Murphy K. Measurement of OEF and absolute CMRO2: MRI-based methods using interleaved and combined hypercapnia and hyperoxia. In. Neuroimage. 2013:135–147. [PubMed: 23769703]
4. Blockley NP, Griffeth VEM, Simon AB, Buxton RB. A review of calibrated blood oxygenation level-dependent (BOLD) methods for the measurement of task-induced changes in brain oxygen metabolism. 2012

5. Donahue MJ, Dethrage LM, Faraco CC, Jordan LC, Clemmons P, Singer R, Mocco J, Shyr Y, Desai A, O'Duffy A, Riebau D, Hermann L, Connors J, Kirshner H, Strother MK. Routine clinical evaluation of cerebrovascular reserve capacity using carbogen in patients with intracranial stenosis. Stroke. 2014; 45:2335–41. [PubMed: 24938845]

6. Donahue MJ, Ayad M, Moore R, van Osch M, Singer R, Clemmons P, Strother M. Relationships between hypercarbic reactivity, cerebral blood flow, and arterial circulation times in patients with moyamoya disease. J Magn Reson Imaging. 2013; 38:1129–39. [PubMed: 23440909]

7. Jane Taylor N, Baddeley H, Goodchild KA, Powell MEB, Thoumine M, Culver LA, James Stirling J, Saunders MI, Hoskin PJ, Phillips H, Padhani AR, Griffiths JR. BOLD MRI of human tumor oxygenation during carbogen breathing. J Magn Reson Imaging. 2001; 14:156–163. [PubMed: 11477674]

8. Gauthier CJ, Hoge RD. A generalized procedure for calibrated MRI incorporating hyperoxia and hypercapnia. Hum Brain Mapp. 2013; 34:1053–1069. [PubMed: 23015481]

9. Williams DS, Detre JA, Leigh JS, Koretsky AP. Magnetic resonance imaging of perfusion using spin inversion of arterial water. Proc Natl Acad Sci U S A. 1992; 89:212–216. [PubMed: 1729691]

10. Lu H, Clingman C, Golay X, van Zijl PCM. Determining the longitudinal relaxation time (T1) of blood at 3.0 Tesla. Magn Reson Med. 2004; 52:679–82. [PubMed: 15334591]

11. Ma, Y.; Berman, AJL.; Pike, GB. The Effect of Dissolved Oxygen on Relaxation Rates of Blood Plasma. Proceedings 22nd Scientific Meeting International Society for Magnetic Resonance in Medicine; 2014; p. 3099

12. Silvennoinen MJ, Kettunen MI, Kauppinen Ra. Effects of hematocrit and oxygen saturation level on blood spin-lattice relaxation. Magn Reson Med. 2003; 49:568–71. [PubMed: 12594761]

13. Grgac K, van Zijl PCM, Qin Q. Hematocrit and oxygenation dependence of blood (1)H(2)O T(1) at 7 Tesla. Magn Reson Med. 2013; 70:1153–9. [PubMed: 23169066]

14. d'Othée B, Rachmuth G, Munasinghe J, Lang E. The effect of hyperoxygenation on T1 relaxation time in vitro 1. Acad Radiol. 2003

15. Bulte DP, Chiarelli Pa, Wise RG, Jezzard P. Cerebral perfusion response to hyperoxia. J Cereb Blood Flow Metab. 2007; 27:69–75. [PubMed: 16670698]

16. Zhang X, Petersen ET, Ghariq E, De Vis JB, Webb AG, Teeuwisse WM, Hendrikse J, van Osch MJP. In vivo blood T(1) measurements at 1.5 T, 3 T, and 7 T. Magn Reson Med. 2013; 70:1082–6. [PubMed: 23172845]

17. Varela M, Hajnal JV, Petersen ET, Golay X, Merchant N, Larkman DJ. A method for rapid in vivo measurement of blood T1. NMR Biomed. 2011; 24:80–8. [PubMed: 20669148]

18. Tadamura E, Hatabu H, Li W, Prasad PV, Edelman RR. Effect of oxygen inhalation on relaxation times in various tissues. J Magn Reson Imaging. 1997; 7:220–225. [PubMed: 9039619]

19. Shimada K, Nagasaka T. In vivo Measurement of Longitudinal Relaxation Time of Human Blood by Inversion-recovery Fast Gradient-echo MR Imaging at 3T. Magn Reson Med. 2012; 11:265–271.

20. Heijtel DFR, Mutsaerts HJMM, Bakker E, Schober P, Stevens MF, Petersen ET, van Berckel BNM, Majoie CBLM, Booij J, van Osch MJP, Vanbavel E, Boellaard R, Lammertsma AA, Nederveen AJ. Accuracy and precision of pseudo-continuous arterial spin labeling perfusion during baseline and hypercapnia: a head-to-head comparison with ^{15}O H_2O positron emission tomography. Neuroimage. 2014; 92:182–92. [PubMed: 24531046]

21. Noseworthy MD, Kim JK, Stainsby Ja, Stanisz GJ, Wright Ga. Tracking oxygen effects on MR signal in blood and skeletal muscle during hyperoxia exposure. J Magn Reson Imaging. 1999; 9:814–20. [PubMed: 10373029]

22. Floyd TF, Clark JM, Gelfand R, Detre JA, Ratcliffe S, Guvakov D, Lambertsen CJ, Eckenhoff RG. Independent cerebral vasoconstrictive effects of hyperoxia and accompanying arterial hypocapnia at 1 ATA. J Appl Physiol. 2003; 95:2453–61. [PubMed: 12937024]

23. Sicard KM, Duong TQ. Effects of hypoxia, hyperoxia, and hypercapnia on baseline and stimulus-evoked BOLD, CBF, and CMRO2 in spontaneously breathing animals. Neuroimage. 2005; 25:850–858. [PubMed: 15808985]

24. Pilkinton DT, Hiraki T, Detre JA, Greenberg JH, Reddy R. Absolute cerebral blood flow quantification with pulsed arterial spin labeling during hyperoxia corrected with the simultaneous

measurement of the longitudinal relaxation time of arterial blood. Magn Reson Med. 2012; 67:1556–65. [PubMed: 22135087]

25. Hare HV, Germuska M, Kelly ME, Bulte DP. Comparison of CO2 in air versus carbogen for the measurement of cerebrovascular reactivity with magnetic resonance imaging. J Cereb Blood Flow Metab. 2013; 33:1799–805. [PubMed: 23921896]
26. Donahue MJ, Faraco CC, Strother MK, Chappell Ma, Rane S, Dethrage LM, Hendrikse J, Siero JCW. Bolus arrival time and cerebral blood flow responses to hypercarbia. J Cereb Blood Flow Metab. 2014; 34:1243–52. [PubMed: 24780904]
27. Langdon W, Donahue MJ, van der Kolk AG, Rane S, Strother MK. Correlating hemodynamic magnetic resonance imaging with high-field intracranial vessel wall imaging in stroke. J Radiol Case Rep. 2014; 8:1–10. [PubMed: 25426229]
28. Faraco CC, Strother MK, Dethrage LM, Jordan L, Singer R, Clemmons PF, Donahue MJ. Dual echo vessel-encoded ASL for simultaneous BOLD and CBF reactivity assessment in patients with ischemic cerebrovascular disease. Magn Reson Med. 2015; 73:1579–92. [PubMed: 24757044]
29. Chiarelli PA, Bulte DP, Wise R, Gallichan D, Jezzard P. A calibration method for quantitative BOLD fMRI based on hyperoxia. Neuroimage. 2007; 37:808–20. [PubMed: 17632016]
30. Blockley NP, Griffeth VEM, Simon AB, Dubowitz DJ, Buxton RB. Calibrating the BOLD response without administering gases: Comparison of hypercapnia calibration with calibration using an asymmetric spin echo. Neuroimage. 2014
31. Germuska M, Bulte DP. MRI measurement of oxygen extraction fraction, mean vessel size and cerebral blood volume using serial hyperoxia and hypercapnia. Neuroimage. 2014; 92:132–42. [PubMed: 24531048]
32. Frederick, B.; Tong, Y.; Strother, MK.; Nickerson, L.; Lindsey, K.; Donahue, MJ. Derivation of flow information from a hypocarbia challenge study using time delay correlation processinge. Proc. ISMRM, 21st Annual Meeting; Salt Lake City. 2013; p. 206
33. Ashkanian M, Gjedde A, Mouridsen K, Vafaee M, Hansen KV, Ostergaard L, Andersen G. Carbogen inhalation increases oxygen transport to hypoperfused brain tissue in patients with occlusive carotid artery disease: increased oxygen transport to hypoperfused brain. Brain Res. 2009; 1304:90–5. [PubMed: 19782665]
34. Lu H, Golay X, Pekar JJ, Van Zijl PCM. Functional magnetic resonance imaging based on changes in vascular space occupancy. Magn Reson Med. 2003; 50:263–274. [PubMed: 12876702]
35. Donahue MJ, van Laar PJ, van Zijl PCM, Stevens RD, Hendrikse J. Vascular space occupancy (VASO) cerebral blood volume-weighted MRI identifies hemodynamic impairment in patients with carotid artery disease. J Magn Reson Imaging. 2009; 29:718–724. [PubMed: 19243067]
36. Xu F, Liu P, Pascual JM, Xiao G, Lu H. Effect of hypoxia and hyperoxia on cerebral blood flow, blood oxygenation, and oxidative metabolism. J Cereb Blood Flow Metab. 2012; 32:1909–18. [PubMed: 22739621]
37. Zaharchuk G, Martin AJ, Dillon WP. Noninvasive imaging of quantitative cerebral blood flow changes during 100% oxygen inhalation using arterial spin-labeling MR imaging. AJNR Am J Neuroradiol. 2008; 29:663–7. [PubMed: 18397966]
38. Donahue MJ, Strother MK, Hendrikse J. Novel MRI approaches for assessing cerebral hemodynamics in ischemic cerebrovascular disease. Stroke. 2012; 43:903–915. [PubMed: 22343644]
39. MacIntosh BJ, Lindsay AC, Kylintireas I, Kuker W, Günther M, Robson MD, Kennedy J, Choudhury RP, Jezzard P. Multiple inflow pulsed arterial spin-labeling reveals delays in the arterial arrival time in minor stroke and transient ischemic attack. Am J Neuroradiol. 2010; 31:1892–1894. [PubMed: 20110375]
40. Jenkinson M, Smith S. A global optimisation method for robust affine registration of brain images. Med Image Anal. 2001; 5:143–156. [PubMed: 11516708]
41. Alsop DC, Detre JA, Golay X, Günther M, Hendrikse J, Hernandez-Garcia L, Lu H, Macintosh BJ, Parkes LM, Smits M, van Osch MJP, Wang DJJ, Wong EC, Zaharchuk G. Recommended implementation of arterial spin-labeled perfusion MRI for clinical applications: A consensus of the ISMRM perfusion study group and the european consortium for ASL in dementia. Magn Reson Med. 2015; 73:102–116.

42. Van Osch MJP, Teeuwisse WM, van Walderveen MAA, Hendrikse J, Kies DA, van Buchem MA. Can arterial spin labeling detect white matter perfusion signal? Magn Reson Med. 2009; 62:165–73. [PubMed: 19365865]

43. Samuels OB, Joseph GJ, Lynn MJ, Smith HA, Chimowitz MI. A standardized method for measuring intracranial arterial stenosis. AJNR Am J Neuroradiol. 2000; 21:643–646. [PubMed: 10782772]

44. Taylor DW, Whisnant JP. Collaborators NAS ic CET. Beneficial Effect of Carotid Endarterectomy in Symptomatic Patients with High-Grade Stenosis. N Engl J Med. 1991; 115:34.

45. Haddock B, Larsson HBW, Hansen AE, Rostrup E. Measurement of brain oxygenation changes using dynamic T(1)-weighted imaging. Neuroimage. 2013; 78:7–15. [PubMed: 23578574]

46. Rostrup E, Larsson HBW, Toft PB, Garde K, Henriksen O. Signal changes in gradient echo images of human brain induced by hypo- and hyperoxia. NMR Biomed. 1995; 8:41–47. [PubMed: 7547184]

47. Watson NA, Beards SC, Altaf N, Kassner A, Jackson A. The effect of hyperoxia on cerebral blood flow: a study in healthy volunteers using magnetic resonance phase-contrast angiography. Eur J Anaesthesiol. 2000; 17:152–9. [PubMed: 10758463]

48. Aslan S, Xu F, Wang PL, Uh J, Yezhuvath US, van Osch M, Lu H. Estimation of labeling efficiency in pseudocontinuous arterial spin labeling. Magn Reson Med. 2010; 63:765–71. [PubMed: 20187183]

49. Faraco CC, Strother MK, Siero JC, Arteaga DF, Scott AO, Jordan LC, Donahue MJ. The cumulative influence of hyperoxia and hypercapnia on blood oxygenation and R2(.). J Cereb Blood Flow Metab. 201510.1038/jcbfm.2015.168

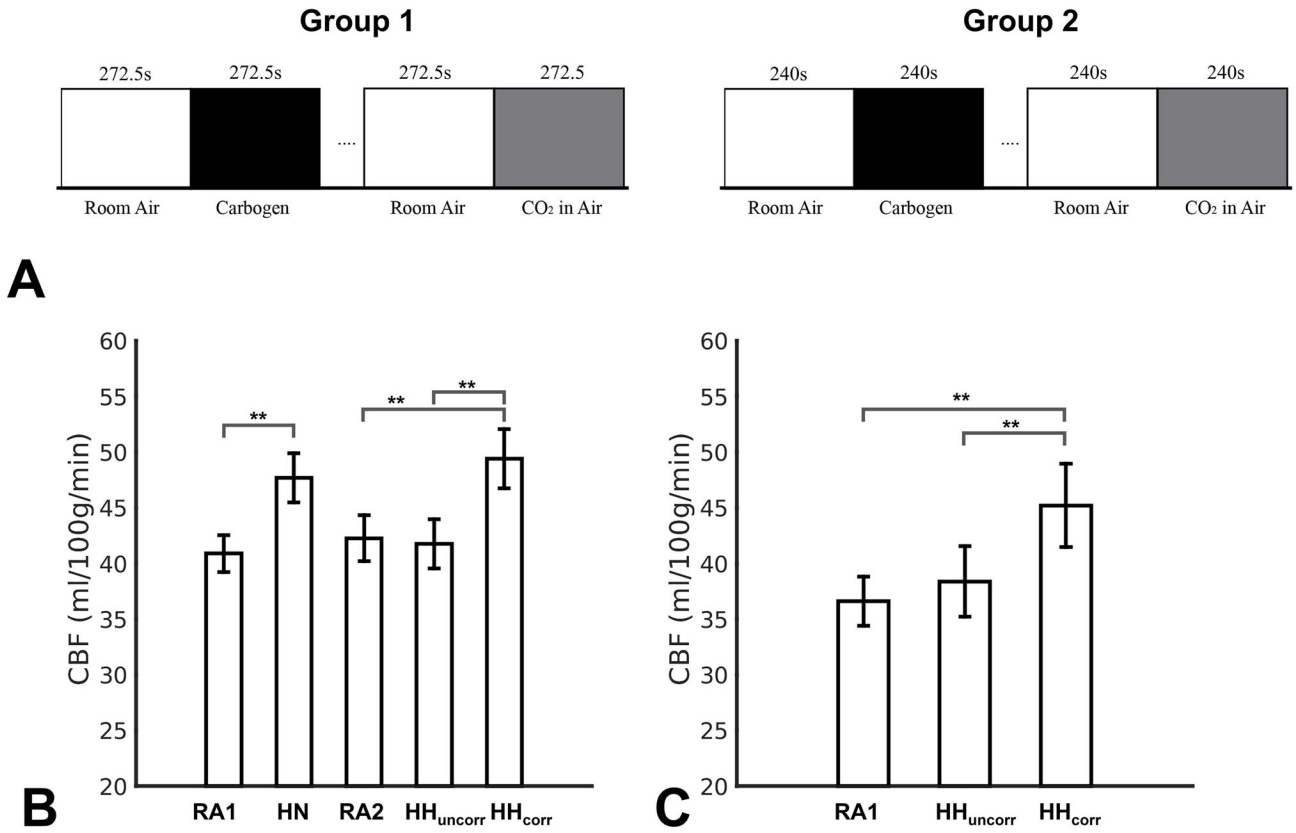

Figure 1.

(A) Experimental paradigm. Each 272.5s (group1, left) and 240s (group2, right) presentation of a gas mixture (e.g., room air, carbogen or CO_2 in air) was a stimulus block. The presentation order of the scanning blocks (e.g., Room air + hypercarbic stimulus block) was randomized across healthy participants, where the space between scanning blocks signifies monitored time for the participant's heart rate, Y_a, and $EtCO_2$ to return to baseline. Mean CBF values for healthy participants **(B)** and patients **(C)** for different gas mixtures: room air (RA1) before 5%CO_2 in air (HN), room air (RA2) before carbogen-5 (HH). HH_{uncorr} and HH_{corr} are the CBF values for HH condition using a normoxic $T_{1a,RA}$ (1.65s) and hyperoxic $T_{1a,HH}$ (1.49s) obtained from the fitting procedure. Error bars denote the s.e.m. (n=14 control volunteers and n=10 steno-occlusive disease patients). ** denotes significant differences ($p < 0.025$) for a paired Student's t-test.

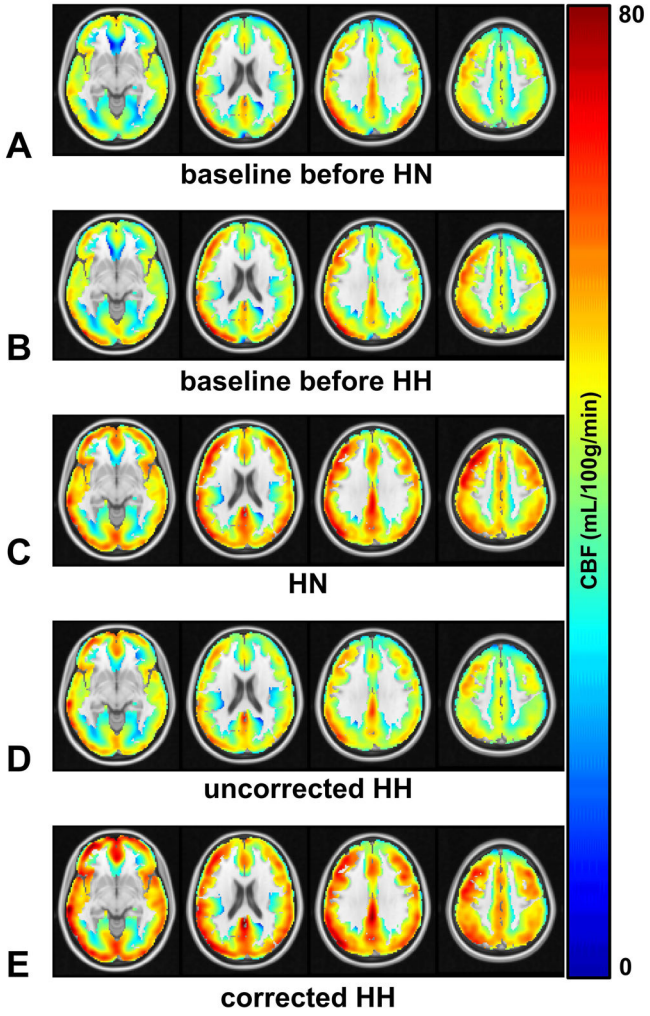

Figure 2.

Mean CBF maps (ml/100g tissue/min) for healthy participants during **(A)** baseline before 5%CO_2 in air (HN), **(B)** baseline before carbogen-5 (HH), **(C)** 5%CO_2 in air (HN), **(D)** uncorrected carbogen-5 (HH), $T_{1a,HH} = T_{1a,RA} = 1.65$s, and **(E)** corrected carbogen-5 (HH), calculated $T_{1a,HH} = 1.49$s.

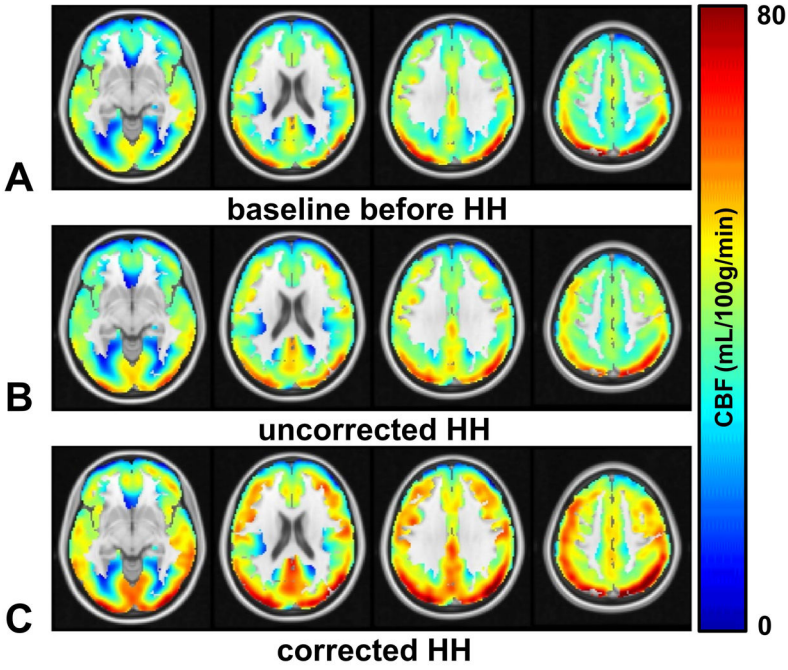

Figure 3.

Mean CBF maps (ml/100g tissue/min) for patients during **(A)** baseline before carbogen-5 (HH), **(B)** uncorrected carbogen-5 (HH), $T_{1a,HH} = T_{1a,RA} = 1.65$s, and **(C)** corrected carbogen-5 (HH), calculated $T_{1a,HH} = 1.49$s. Owing to multiple vessels with steno-occlusive disease, patients have not been oriented by flow-limiting hemisphere.

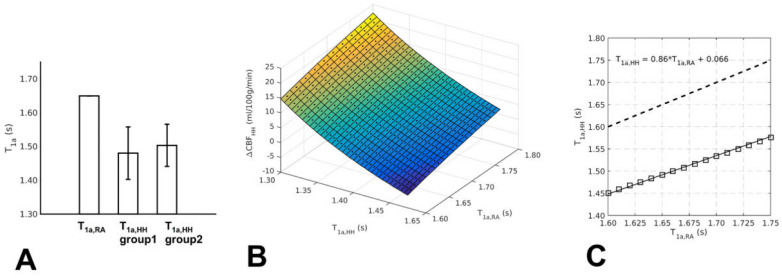

Figure 4.

$T_{1a,HH}$ calculation results. **(A)** Reduced $T_{1a,HH}$ was found for both groups as compared to the normoxic condition (left bar, $T_{1a,RA}$ = 1.65s); 1.48s and 1.50s for group 1 and group 2, respectively, yielding a combined result of $T_{1a,HH}$ = 1.49s. No significant difference in $T_{1a,HH}$ was found between group 1 and group 2. Error bars denote the s.d. **(B)** Dependency of ΔCBF_{HH} ($CBF_{HH} - CBF_{RA}$) for different calculated hyperoxic $T_{1a,HH}$ and assumed normoxic $T_{1a,RA}$ values. **(C)** Dependency of the calculated $T_{1a,HH}$ for different assumed normoxic $T_{1a,RA}$ values.

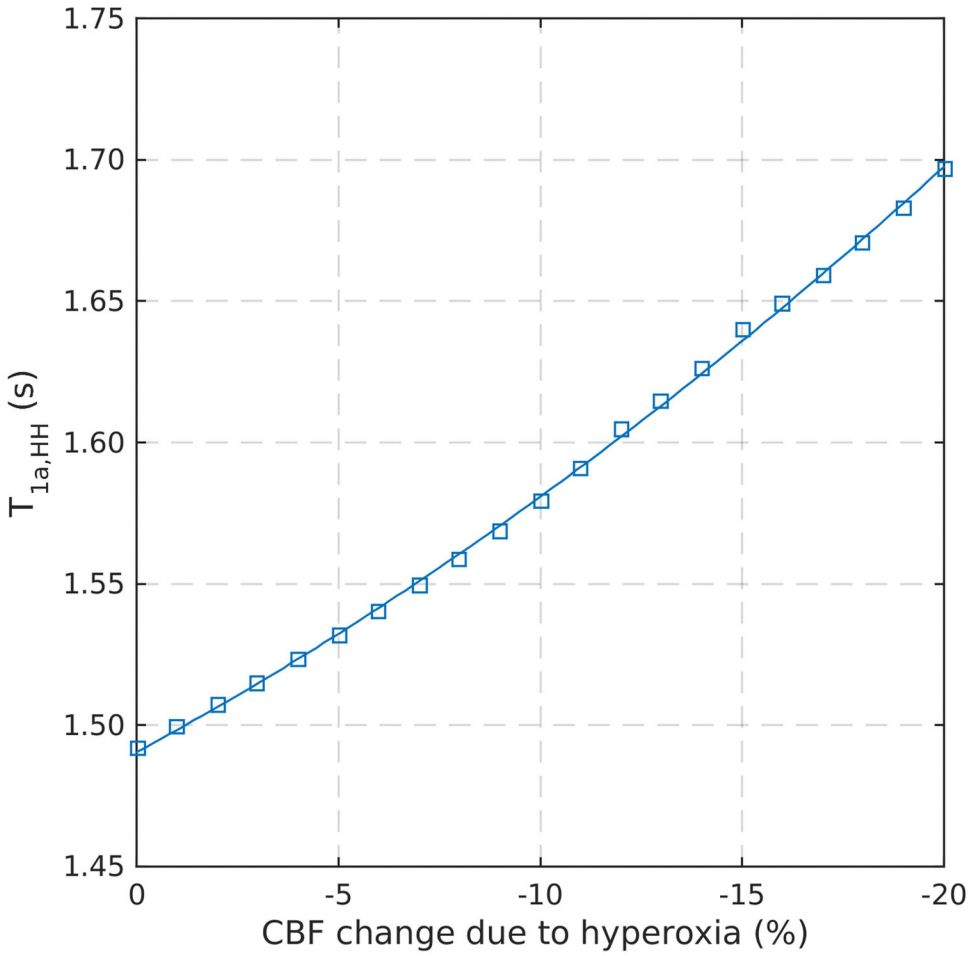

Figure 5.

Simulation demonstrating the effect of small hyperoxic-induced vasoconstriction (0 – 20% CBF reduction) on the arterial blood $T_{1a,HH}$ calculations. Note that for 0% CBF reduction due to hyperoxia the calculated $T_{1a,HH}$ = 1.49s as shown in Figure 4A. For larger potential vasoconstrictive effects due to hyperoxia (more CBF reduction) the calculated $T_{1a,HH}$ will increase accordingly. For a CBF reduction of ~16% the $T_{1a,HH}$ approaches the normoxic value $T_{1a,RA}$ = 1.65s, which is the same percentage difference between the corrected and uncorrected carbogen-5 (HH) CBF values in Figure 1A as expected.

Table 1

Summary of All Data from Patients

Patient ID	Age (yrs)	Sex	Stenosis Location (% stenosis)	Room Air CBF (ml/100g tissue/min)	Carbogen-5 CBF (ml/100g tissue/min) Uncorrected (T_{1a} = = 1.65s)	Carbogen-5 CBF (ml/100g tissue/min) Corrected (T_{1a} = 1.49s)
1	72	M	Right Paraclinoid ICA (53%); Right IC vertebral (67%)	48.1 ± 19.5	52.1 ± 22.2	61.4 ± 26.2
2	66	M	Right MCA (28%); Left MCA (59%); Right IC vertebral (57%)	32.2 ± 15.7	34.8 ± 16.5	41.0 ± 19.5
3	82	F	Left MCA (33%); Right MCA (65%)	26.4 ± 15.3	31.1 ± 14.6	36.7 ± 17.3
4	64	M	Left Paraclinoid ICA (33%); Right cervical vertebral (68%)	31.0 ± 10.5	27.7 ± 10.9	32.6 ± 12.8
5	72	F	Right MCA (67%)	35.3 ± 12.4	37.1 ± 13.0	43.8 ± 15.4
6	73	F	Right MCA (73%); Left MCA (46%)	44.6 ± 14.4	42.8 ± 17.1	50.3 ± 20.2
7	38	F	Left MCA (68%)	49.7 ± 21.1	64.1 ± 25.4	75.6 ± 30.1
8	62	M	Left ICA (100%); Right cervical vertebral (80%)	30.9 ± 18.2	26.5 ± 15.4	31.2 ± 18.1
9	51	M	Right MCA (79%)	29.4 ± 11.5	30.1 ± 11.5	35.5 ± 13.6
10	69	M	Right MCA (99%); Right ICA (99%); Right cervical vertebral (76%)	38.6 ± 13.0	37.4 ± 13.9	44.0 ± 16.3
Mean	61.4±13.3			36.6 ± 8.3	38.4 ± 11.8	45.2 ± 13.9